

Electronic Supplementary Information

Antimony doped lead-free double perovskites ($\text{Cs}_2\text{NaBi}_{1-x}\text{Sb}_x\text{Cl}_6$) with enhanced light absorption and tunable emission

Shufang Wu,^{1,2} Wenbo Li,^{1,2,3} Junjie Hu,^{1,2,4} and Peng Gao^{1,2,4*}

¹CAS Key Laboratory of Design and Assembly of Functional Nanostructures, and Fujian Key Laboratory of Nanomaterials, Fujian Institute of Research on the Structure of Matter, Chinese Academy of Sciences, Fuzhou, Fujian 350002, China

²Laboratory of Advanced Functional Materials, Xiamen Institute of Rare Earth Materials, Haixi Institute, Chinese Academy of Sciences, Xiamen 361021, China

³Faculty of Materials Metallurgy and Chemistry, Jiangxi University of Science and Technology, Ganzhou, Jiangxi 341000, China

⁴University of Chinese Academy of Sciences, Beijing 100049, China

*Correspondence: peng.gao@fjirsm.ac.cn; Tel: 0592-359-4003

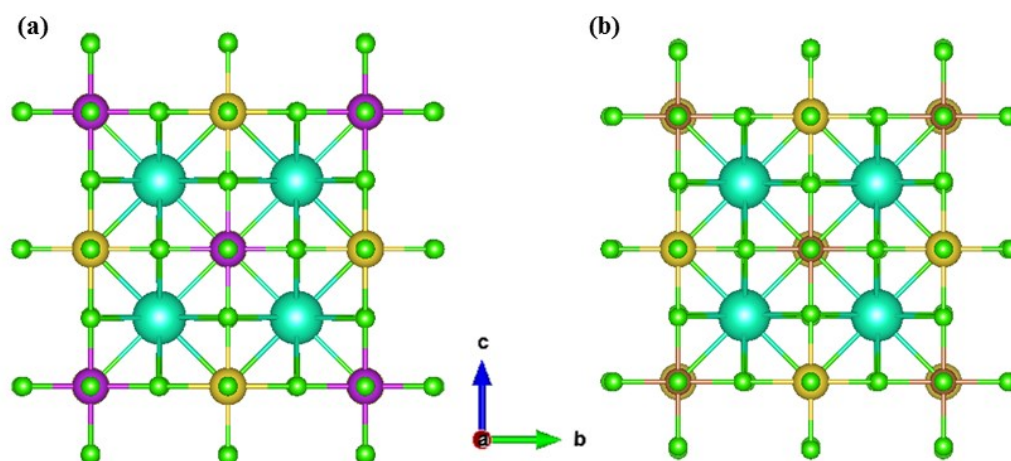


Fig. S1. The supercells of $\text{Cs}_2\text{NaBiCl}_6$ (a) and $\text{Cs}_2\text{NaSbCl}_6$ (b) for computational calculation. Cs atoms, cyan; Na atoms, yellow; Bi atoms, violet; Sb atoms, brown; Cl atoms, green.

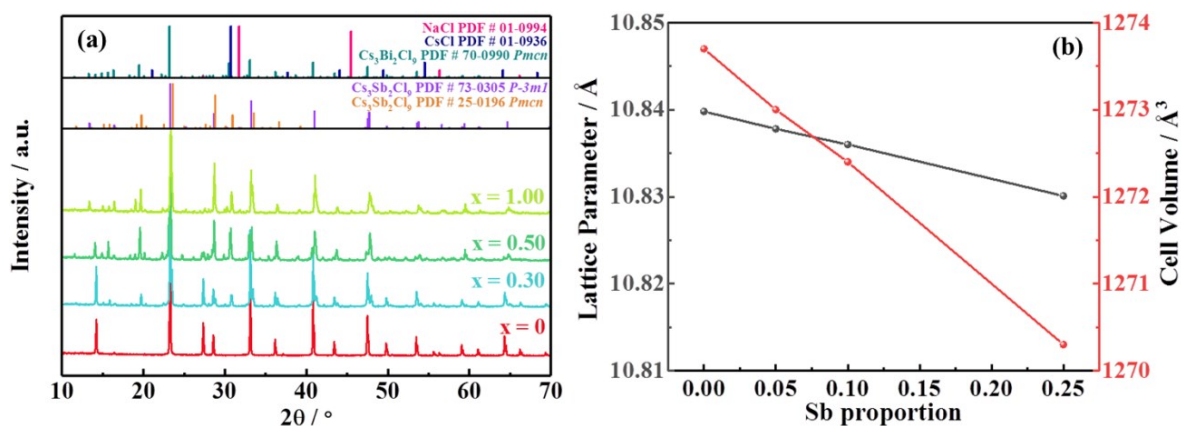


Fig. S2. a) The enlarged XRD patterns of $\text{Cs}_2\text{NaBi}_{1-x}\text{Sb}_x\text{Cl}_6$ ($x = 0, 0.3, 0.5$ and 1.0). $\text{Cs}_3\text{Sb}_2\text{Cl}_9$, CsCl , NaCl and other by-products are produced when $x \geq 0.3$. b) The variation of cubic crystal lattice parameter and cell volume, as a function of Sb^{3+} substitution proportion. The values of lattice parameter and cell volume are derived by using the Rietveld method.

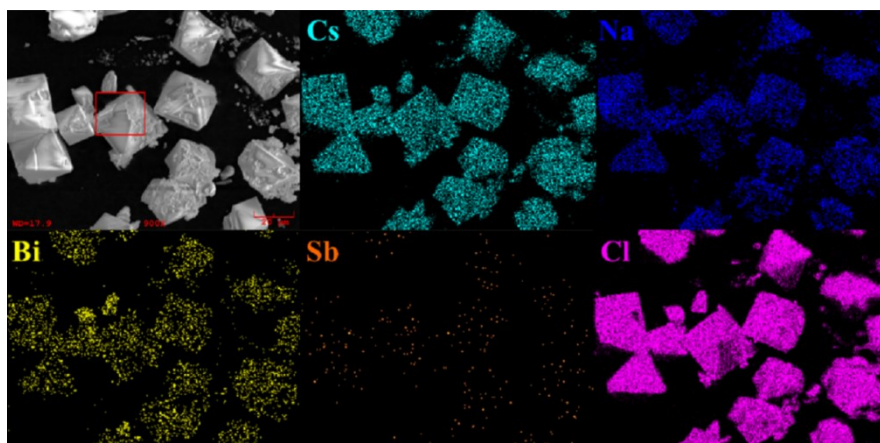


Fig. S3. EDS elemental mapping of Cs, Na, Bi, Sb and Cl elements in $\text{Cs}_2\text{NaBi}_{0.95}\text{Sb}_{0.05}\text{Cl}_6$ double perovskite microcrystals.

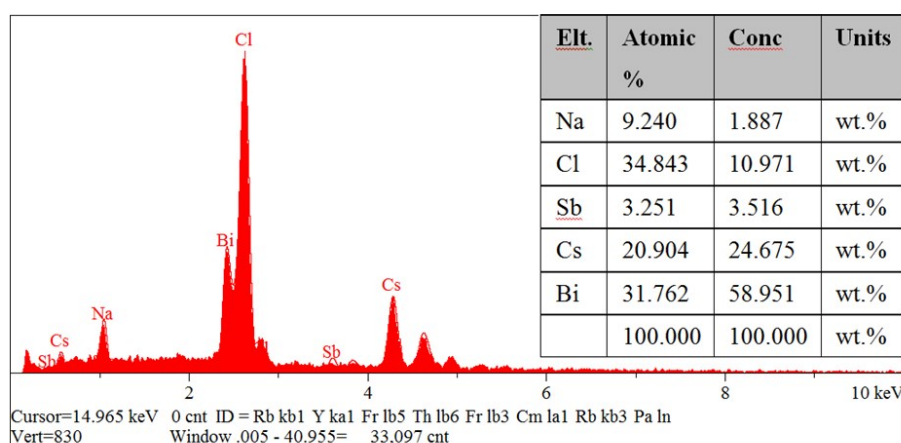


Fig. S4. EDS spectra for $\text{Cs}_2\text{NaBi}_{0.95}\text{Sb}_{0.05}\text{Cl}_6$ double perovskite microcrystals. The inset table presents the corresponding approximate element quantification.

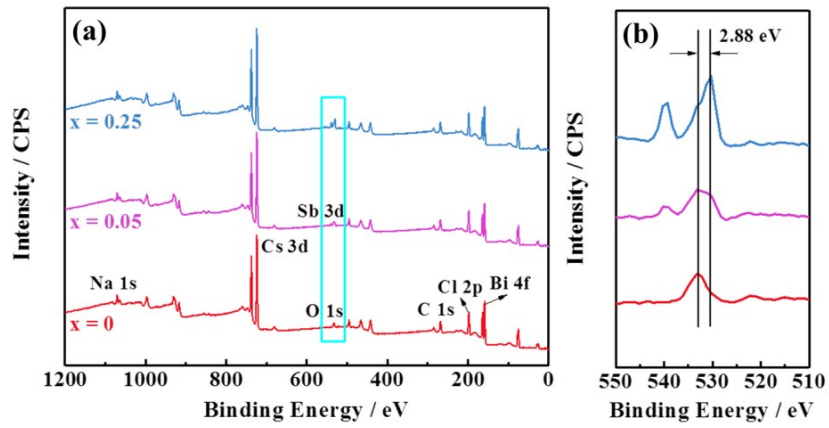


Fig. S5. XPS survey spectra (a), and the amplified peaks attributed to O 1s and Sb 3d (b) of $\text{Cs}_2\text{NaBi}_{1-x}\text{Sb}_x\text{Cl}_6$ ($x = 0, 0.05$ and 0.25).

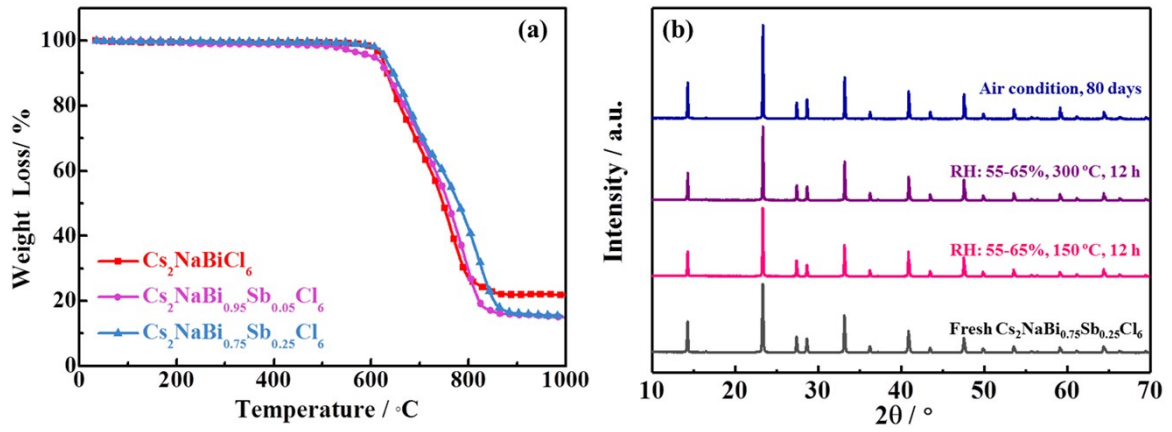


Fig. S6. (a) TGA data for $\text{Cs}_2\text{NaBi}_{1-x}\text{Sb}_x\text{Cl}_6$ ($x = 0, 0.05$ and 0.25). (b) PXRD patterns of $\text{Cs}_2\text{NaBi}_{0.75}\text{Sb}_{0.25}\text{Cl}_6$ measured under different conditions.

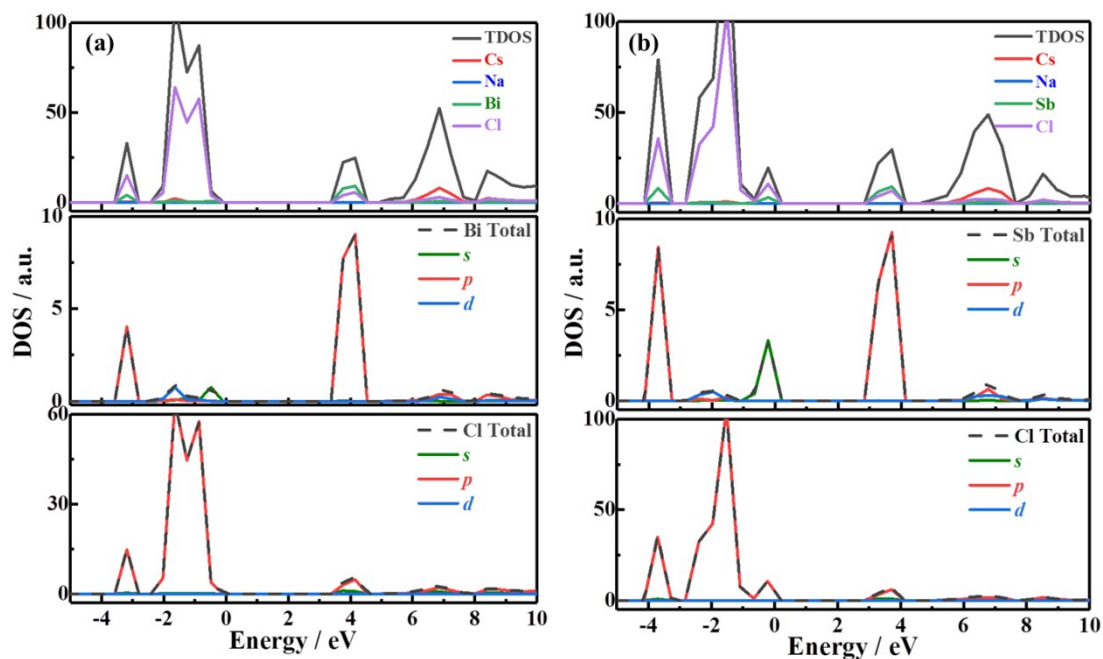


Fig. S7. Electronic density of states (DOS) for $\text{Cs}_2\text{NaBiCl}_6$ (a) and $\text{Cs}_2\text{NaSbCl}_6$ (b).

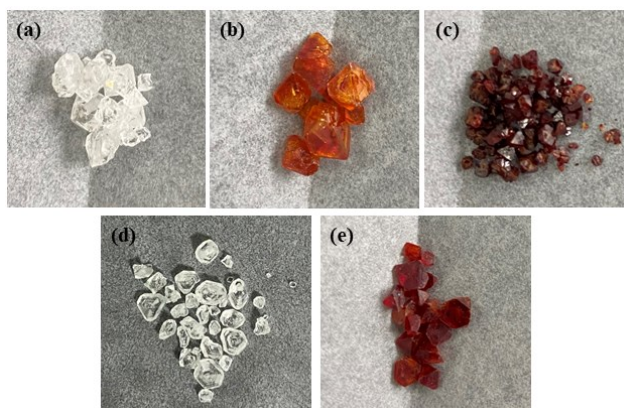


Fig. S8. Pictures for the crystals of $\text{Cs}_2\text{NaBiCl}_6$ (a, d), $\text{Cs}_2\text{NaBi}_{0.95}\text{Sb}_{0.05}\text{Cl}_6$ (b, e), and $\text{Cs}_2\text{NaBi}_{0.9}\text{Sb}_{0.1}\text{Cl}_6$ (c) and $\text{Cs}_2\text{NaBi}_{0.95}\text{Sb}_{0.05}\text{Cl}_6$ (d) under daylight, prepared from the reaction solution with adding 3 μl HNO_3 (a-c) or 5 μl H_2O_2 (d, e).

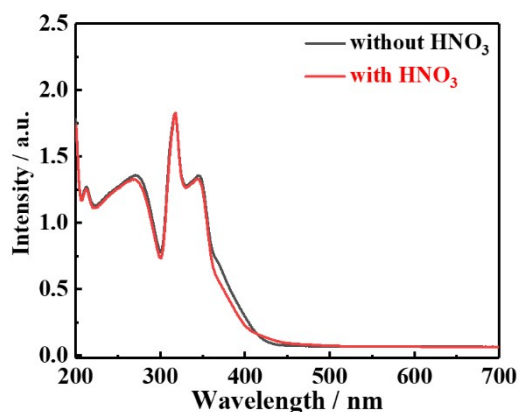


Fig. S9. Steady-state absorption spectra of CsNaBiCl_6 without and with HNO_3 (3 μl) in the hydrothermal reaction.

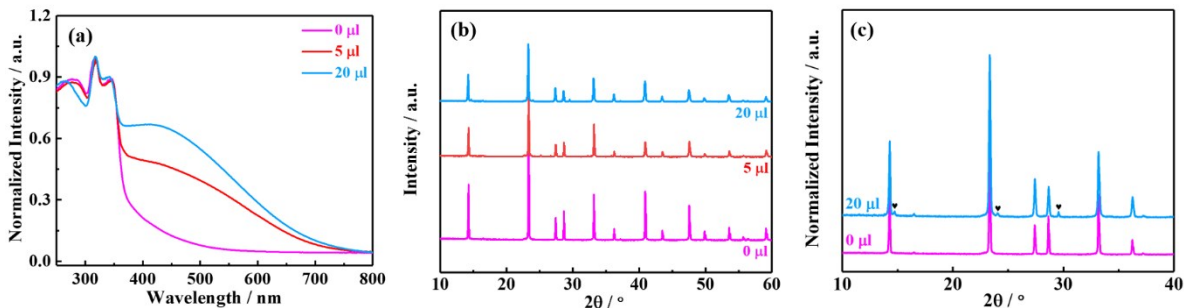


Fig. S10. Steady-state absorption spectra (a), PXRD patterns (b) and the normalized XRD patterns (c) of $\text{Cs}_2\text{NaBi}_{0.95}\text{Sb}_{0.05}\text{Cl}_6$ double perovskites with different amounts of H_2O_2 added in the hydrothermal reaction. Some weak diffraction peaks (marked with the symbol ♥) that can be indexed to $\text{Cs}_2\text{Bi}_{0.5}\text{Sb}_{0.5}\text{Cl}_6$, are also observed in $\text{Cs}_2\text{NaBi}_{0.95}\text{Sb}_{0.05}\text{Cl}_6$ crystals prepared by adding 20 μl H_2O_2 .

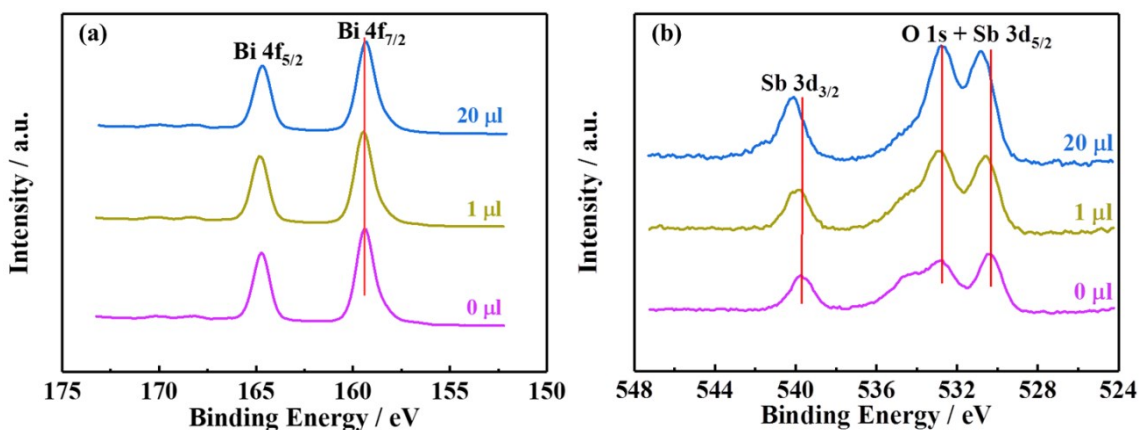


Fig. S11. Bi 4f (a) and Sb 3d (b) XPS spectra for $\text{Cs}_2\text{NaBi}_{0.95}\text{Sb}_{0.05}\text{Cl}_6$ with different amounts of diluted HNO_3 added in the hydrothermal reaction.

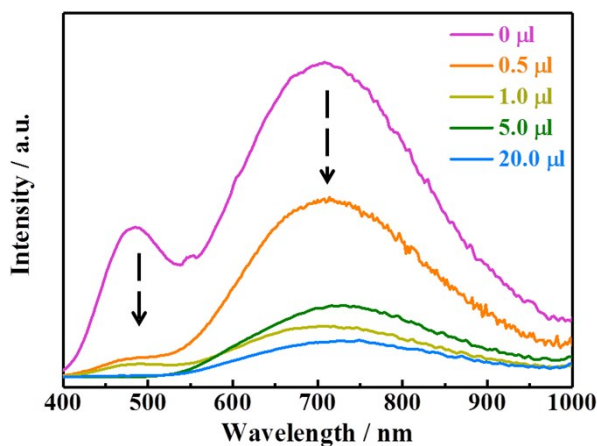


Fig. S12. PL spectra of $\text{Cs}_2\text{NaBi}_{0.95}\text{Sb}_{0.05}\text{Cl}_6$ double perovskites with different amounts of diluted HNO_3 added in the hydrothermal reaction.

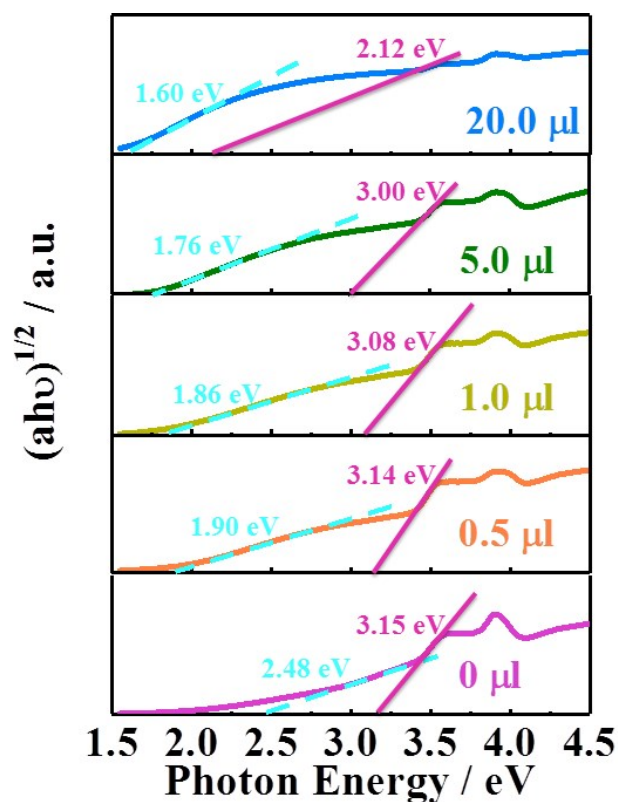


Fig. S13. Tauc plots of $\text{Cs}_2\text{NaBi}_{0.95}\text{Sb}_{0.05}\text{Cl}_6$ double perovskites with different amounts of diluted HNO_3 added in the hydrothermal reaction. The band-gap values are extracted by linear fitting to indirect band-gap Tauc plots.

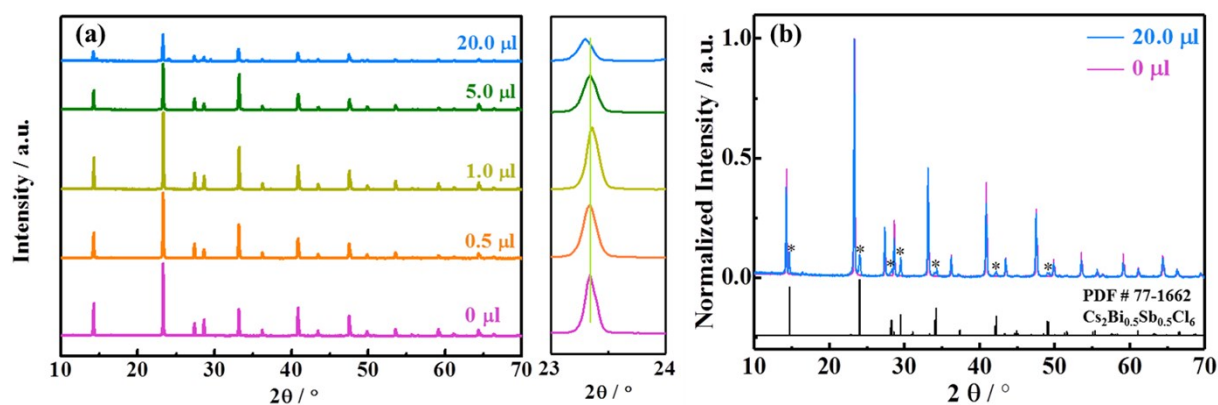


Fig. S14. The effect of adding diluted HNO_3 in the hydrothermal reaction on the crystal structure. a) PXRD patterns and the enlarged diffraction peaks between $23^\circ \sim 24^\circ$ of $\text{Cs}_2\text{NaBi}_{0.95}\text{Sb}_{0.05}\text{Cl}_6$ double perovskites with different amounts of diluted HNO_3 . b) The normalized XRD patterns of $\text{Cs}_2\text{NaBi}_{0.95}\text{Sb}_{0.05}\text{Cl}_6$ with 0 μl and 20 μl diluted HNO_3 . Second phase was observed in $\text{Cs}_2\text{NaBi}_{0.95}\text{Sb}_{0.05}\text{Cl}_6$ crystals with 20 μl diluted HNO_3 .

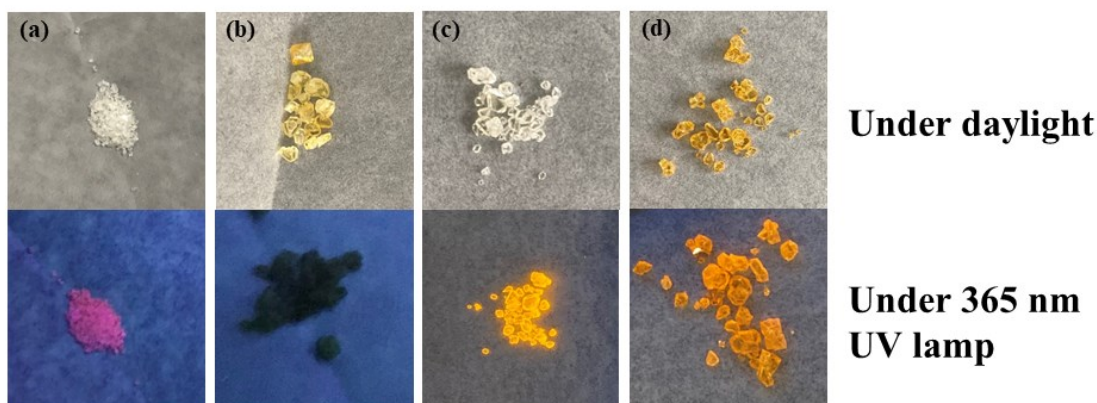


Fig. S15. Pictures for the as-prepared crystals of $\text{Cs}_2\text{NaBiCl}_6$ (a), $\text{Cs}_2\text{NaBi}_{0.75}\text{Sb}_{0.25}\text{Cl}_6$ (b), Mn^{2+} doped $\text{Cs}_2\text{NaBiCl}_6$ (c), and Mn^{2+} doped $\text{Cs}_2\text{NaBi}_{0.75}\text{Sb}_{0.25}\text{Cl}_6$ (d) under daylight (upper) and 365 nm UV light (bottom). The input mole ratio of $\text{Mn}^{2+}/\text{Na}^+$ in Mn^{2+} doped crystals is 0.2.

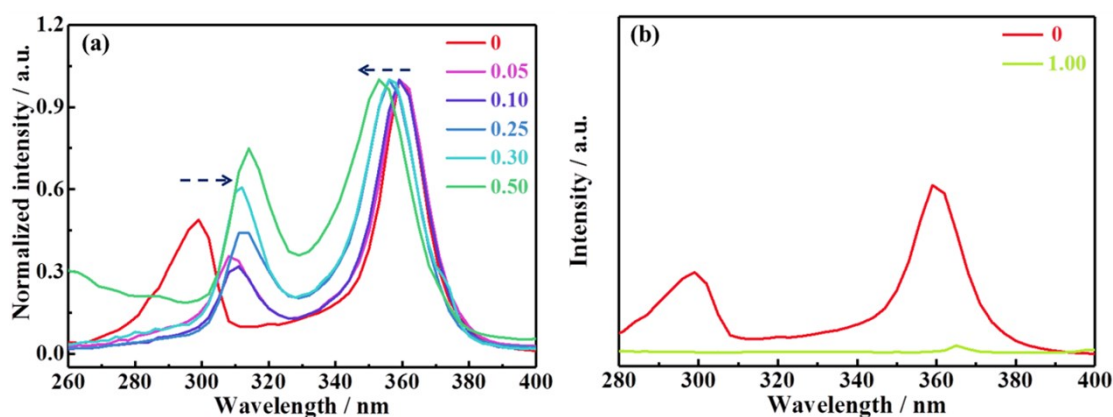


Fig. S16. (a) Photoluminescence excitation spectra (PLE) of $\text{Cs}_2\text{NaBi}_{1-x}\text{Sb}_x\text{Cl}_6$ monitored at 480 nm excepting $\text{Cs}_2\text{NaBiCl}_6$ (at 700 nm). (b) The comparison of the PLE curves for $\text{Cs}_2\text{NaBiCl}_6$ and $\text{Cs}_2\text{NaSbCl}_6$.

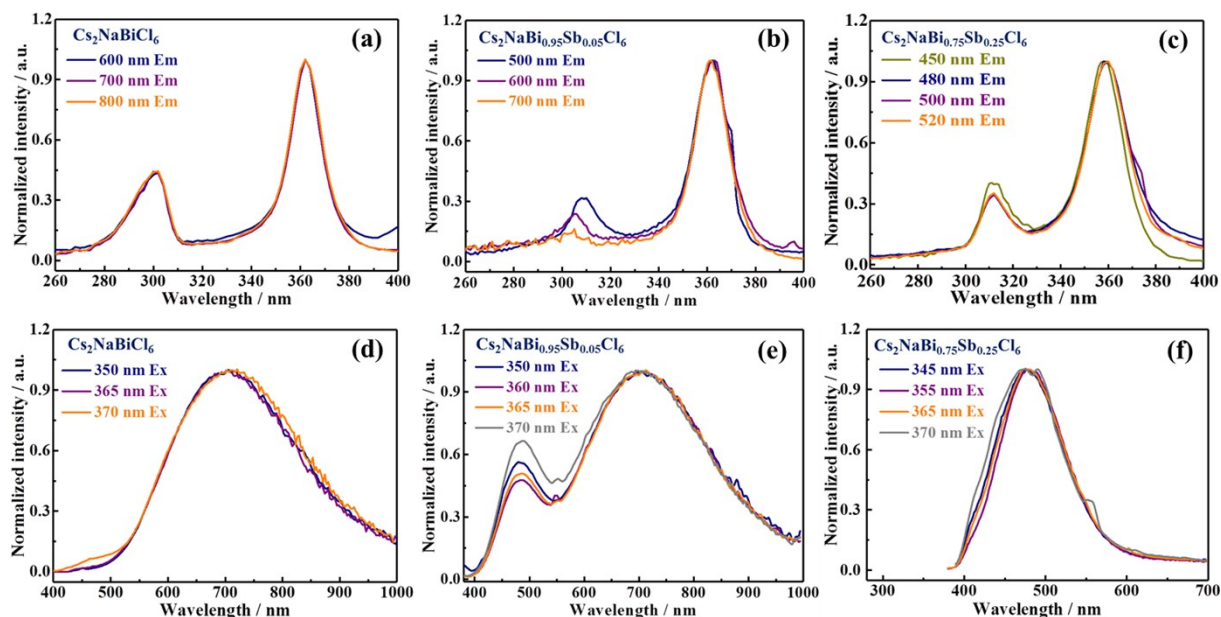


Fig. S17. Emission-wavelength-dependent PLE (a-c) and excitation-wavelength-dependent PL (d-f) spectra of $\text{Cs}_2\text{NaBiCl}_6$ (a, d), $\text{Cs}_2\text{NaBi}_{0.95}\text{Sb}_{0.05}\text{Cl}_6$ (b, e), and $\text{Cs}_2\text{NaBi}_{0.75}\text{Sb}_{0.25}\text{Cl}_6$ (c, f).

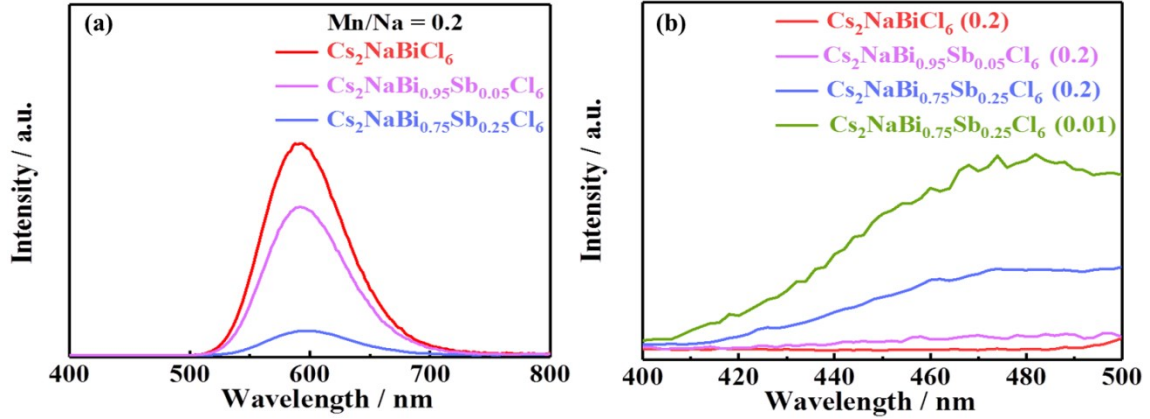


Fig. S18. PL spectra for Mn^{2+} doped $\text{Cs}_2\text{NaBi}_{1-x}\text{Sb}_x\text{Cl}_6$ ($x = 0, 0.05$ and 0.25) with emission peaks centered at 590 nm (a), and 480 nm with amplifying intensity (b). The input mole ratio of $\text{Mn}^{2+}/\text{Na}^+$ in samples is 0.2 or 0.01.

Table S1 Elemental analysis of $\text{Cs}_2\text{NaBi}_{1-x}\text{Sb}_x\text{Cl}_6$ measured by ICP-OES.

samples	Mass Concentration (mg / mL)			Molar Ratio	
	Na	Bi	Sb	Bi/Na	Sb/Na
$\text{Cs}_2\text{NaBiCl}_6$	13.98	119.69	---	0.94	---
$\text{Cs}_2\text{NaBi}_{0.95}\text{Sb}_{0.05}\text{Cl}_6$	15.27	138.61	2.29	0.998	0.03
$\text{Cs}_2\text{NaBi}_{0.9}\text{Sb}_{0.1}\text{Cl}_6$	15.03	273.37	8.86	0.86	0.05
$\text{Cs}_2\text{NaBi}_{0.75}\text{Sb}_{0.25}\text{Cl}_6$	34.92	97.44	8.66	0.71	0.11
$\text{Cs}_2\text{NaBi}_{0.7}\text{Sb}_{0.3}\text{Cl}_6$	6.36	54.97	11.23	0.95	0.33
$\text{Cs}_2\text{NaBi}_{0.5}\text{Sb}_{0.5}\text{Cl}_6$	1.68	28.51	26.10	1.87	2.93
$\text{Cs}_2\text{NaSbCl}_6$	1.11	---	65.09	---	11.06
$\text{Cs}_2\text{NaBiSb}_{0.05}\text{Cl}_6$ (with 20 ml HNO_3)	15.14	151.22	2.98	1.11	0.04

Table S2 Carrier lifetime derived from the decay curves of PL by fitting with bi-exponentials.

Wavelength	sample	τ_1/ns	A_1	τ_2/ns	A_2	Average τ/ns
700 nm	$\text{Cs}_2\text{NaBiCl}_6$	1.82	0.54	5.69	0.43	3.54
	$\text{Cs}_2\text{NaBi}_{0.95}\text{Sb}_{0.05}\text{Cl}_6$	1.97	1.03	12.13	0.07	2.62
480 nm	$\text{Cs}_2\text{NaBi}_{0.95}\text{Sb}_{0.05}\text{Cl}_6$	2.67	0.85	14.06	0.15	4.38
	$\text{Cs}_2\text{NaBi}_{0.75}\text{Sb}_{0.25}\text{Cl}_6$	2.21	1.08	14.58	0.04	2.60

Average τ is calculated according to the equation: Average $\tau = (A_1\tau_1 + A_2\tau_2) / (A_1 + A_2)$